Terrain determinants of permafrost active layer thermal conditions: a case study from Arctic non--glaciated catchment (Bratteggdalen, SW Spitsbergen)

Marek Kasprzak
Institute of Geography and Regional Development
University of Wrocław
Wrocław, Poland
marek.kasprzak@uwr.edu.pl

Mariusz Szymanowski
Institute of Geography and Regional Development
University of Wrocław
Wrocław, Poland
mariusz.szymanowski@uwr.edu.pl

Abstract—**The article concerns the thermal state of permafrost active layer in unglaciated areas of high latitudes (Brattegg valley, SW Spitsbergen). The basic material are data from a network of thermistors located in a drainage basin, including its highest elevations. Measured data were used to search for terrain determinants of ground thermics, expressed by common land surface parameters derived from 20×20 m DTM and surface area temperature obtained from the LANDSAT 8 scene processing. Correlation and regression analysis was used to build models of spatial distribution of ground temperature at different depths. The obtained results show, among others, that temperatures near the ground surface (from 0 to –5 cm) are not significantly correlated with any of the tested topographic parameters, and thus depend on the local features of the ground. An expression of this is the strong dependence of temperature in near subsurface (up to depth 20 cm) on surface temperatures estimated from satellite data. From 10 cm below the surface and deeper, there is a significant negative correlation of temperature with elevation: initially stronger with altitude, and at 100 and 150 cm depth – with relative height.**

I.   Introduction

In the High-Arctic environment, the presence and functioning of permafrost active layer determines the dynamics of hydrological and geomorphological processes. Unfortunately, spatial modelling of ground thermics encounters obstacles resulting not only from the difficulty in determining weight of interactions of interdependent environmental factors, but also on the deficit of measurement data [1, 2]. Technical difficulties and costs of drilling in frozen ground mean that the majority of temperature measurements carried out (eg within the GTN-P network – the Global Terrestrial Network for Permafrost) are often limited to individual boreholes or transects in mountains. This type of data deficiency also applies to Svalbard. Thermal data of the ground in this area are obtained mainly from boreholes located on elevated marine terraces [3–7]. Facing this

situation, an attempt was made to comprehensively diagnose the thermal situation of the ground in one of unglaciated valleys on the west coast of Spitsbergen – the Brattegg valley (φ 77°03'26"N, λ 15°12'59"E), where the ground thermics is measured by a network of thermistor strings reaching the depth of 1.5 m (Fig. 1). The paper presents first results of research on environmental factors that play the main role in shaping the thermics of shallow subsurface. The aim of the research is to investigate the relationship between ground temperature and selected land surface and energy parameters possible to determine on the basis of DTM or LANDSAT scenes and to build regression models to determine spatial distribution of ground temperature.
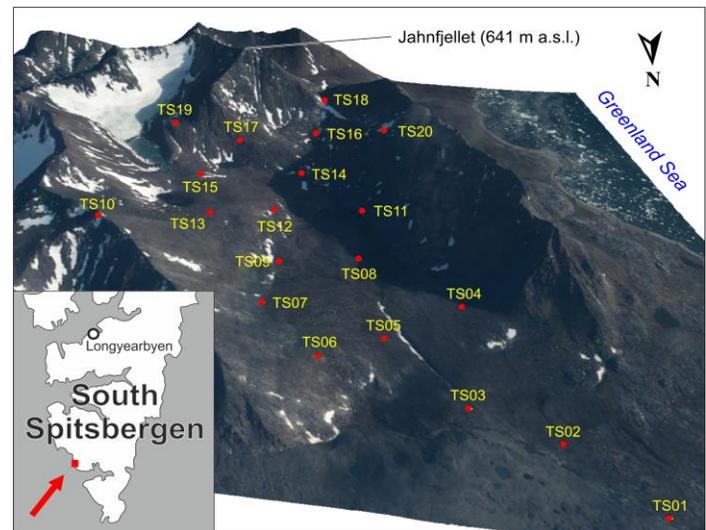

Figure 1.   Perspective view on Brattegg valley and thermistors (TS) positions. SfM-derived digital terrain model obtained from stereographic aerial photographs purchased from Norwegian Polar Institute.

II.   DATA AND METHODS

A. Ground temperature measurement sites

For the needs of the research, a network of 20 ground thermics measurement sites was created, covering the catchment area of the Brattegg River (12.9 km^2). The sites were placed randomly, with an interval of not less than 300 m, in the designated area, where installation works were possible, i.e. excluding the surface of glacial lakes and the steepest sections of slopes (Fig. 1). The measuring stations are made of Geoprecision thermistor strings equipped with mini dataloggers. Temperature measurement is carried out every hour at depths compliant with WMO standards: 0, 5, 10, 20, 50, 100 and 150 cm. Thermistors at 0 cm were placed in protective covers against animals (shaded), and they did not reflect actual thermal conditions of the ground surface. An accuracy of thermistors (typical) is ±0.25 °C. Steps of thermistors installations are schematically given in Fig. 2.

B. Digital data and spatial analysis

The work uses digital data produced by the Norwegian Polar Institute: DTM with a resolution of 20×20 m [8] and stereographic aerial photographs made in 2010, transformed into an orthophotomap in Agisoft PhotoScan software. LANDSAT 8 scene (2017-09-3 11:46 UTC) and the set of tools for automatic retrieval of brightness temperature, land surface emissivity and land surface temperature from LANDSAT data [9] were used to calculate spatial distribution of land surface temperature (LST, Fig. 3). Atmospheric correction was carried out on the basis of Atmospheric Correction Parameter Calculator [10]. QGIS software was used to design the distribution of the measu-rement network (random points inside polygons) and SAGA GIS, ArcGIS and STATISTICA to determine land surface and energy parameters, as well as to carry out further spatial and statistical analysis. The generated parameters are shown in Table 1.

TABLE I.   LAND SURFACE (A) AND SOLAR ENERGETIC (B) PARAMETERS TESTED FOR MODELLING OF GROUND THERMAL CONDITIONS.

A	Elevation (**H**), Valley Depth (**ValDepth**), Channel Network Distance (**VertDist**), Relative Slope Position (**RelSlPos**), Slope (**SL**), Aspect converted by the Cosine function – extreme values (–1, 1) set directions N and S, value 0 directions W and E (**COS_AS**), Profile Curvature (**ProfCurv**), Planar Curvature (**PlanCurv**), TPI radius 100 m (**TPI100**), TPI radius 200 m (**TPI200**), Convergence Index (**Converg**), **LS**, Flow Accumulation (**FlowAcc**), Topographic Wetness Index (**TWI**), Topographic Ruggedness Index (**TRI**)
B	Total solar radiation 3.08.2017 (**TOT215**), Direct solar radiation 3.08.2017 (**DIR215**) Diffuse solar radiation 3.08.2017 (**DIF215**) Duration of direct solar radiation (**DUR215**)
	Land Surface Temperature – Landsat 8, 3 Aug 2017 11:46 (**LST**) NDVI – Landsat 8, 3 Aug 2017 11:46 (**NDVI**)

Figure 2.   Installation of 1.5 m long thermistors string connected to mini datalogger (site TM13, see in Fig. 1, photographs: P. Táborík).
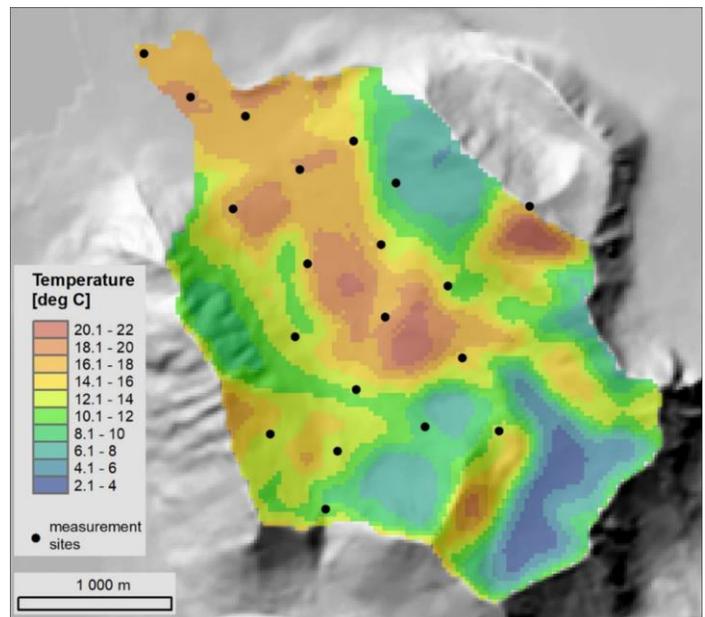

Figure 3.   Land surface temperature (LST) from LANDSAT 8 scene.

C. Modelling of ground temperatures

Spatial distribution of ground temperatures at various depths was examined using regression models. Specification of variables for the model was made using stepwise regression, taking into account elimination of collinear variables. The Multiple Linear Regression (MLR) was then compared to the local Geographically Weighted Regression (GWR) model because there was a suspicion that the spatial process being studied was non-stationary. The choice of the type of the model was made on the basis of comparison of coefficients of determination (R^2 adj.) and standard estimation error size. Autocorrelation of residuals of each model was also tested for the potential use of residual

kriging [11]. The GWR model was chosen for further analysis as better suited. A 48-hour period from August 3, 6:00 to August 5, 5:00 (summer 2017), when the highest ground temperature was recorded on most of measurement sites (for this period it was also possible to obtain the LANDSAT scene), was selected for the analysis. For this period, average temperatures were determined at each of investigated depths.

III.   RESULTS

Testing relationships between average ground temperatures and selected potentially controlling parameters showed the dependence of the upper layer temperature on LST. A significant positive correlation with LST persists to the depth of 50 cm. A significant negative correlation with elevation, expressed both in altitude (H) and in various parameters describing the relative height (VertDist, RelSlPos) is found from the depth of 10 cm. The strength of correlation increases with depth up to 50 cm, and then weakens, but remains still significant and strong (R < −0.5).

Finally, multivariate regression models (MLR and GWR) were built for individual ground depths (Fig. 4). They were specified by the step method with the introduction of significant variables (Table 2). Explanatory (independent) variables, collinear with the previously introduced variables, were removed from the models. For all depths the GWR model turned out to be better fitted to observations (higher coefficient of determination, smaller standard error), which indirectly indicates the nonstation-

TABLE II.   MODELS OF GROUND AVERAGE TEMPERATURES
IN TERM 3RD–5TH AUGUST 2017.

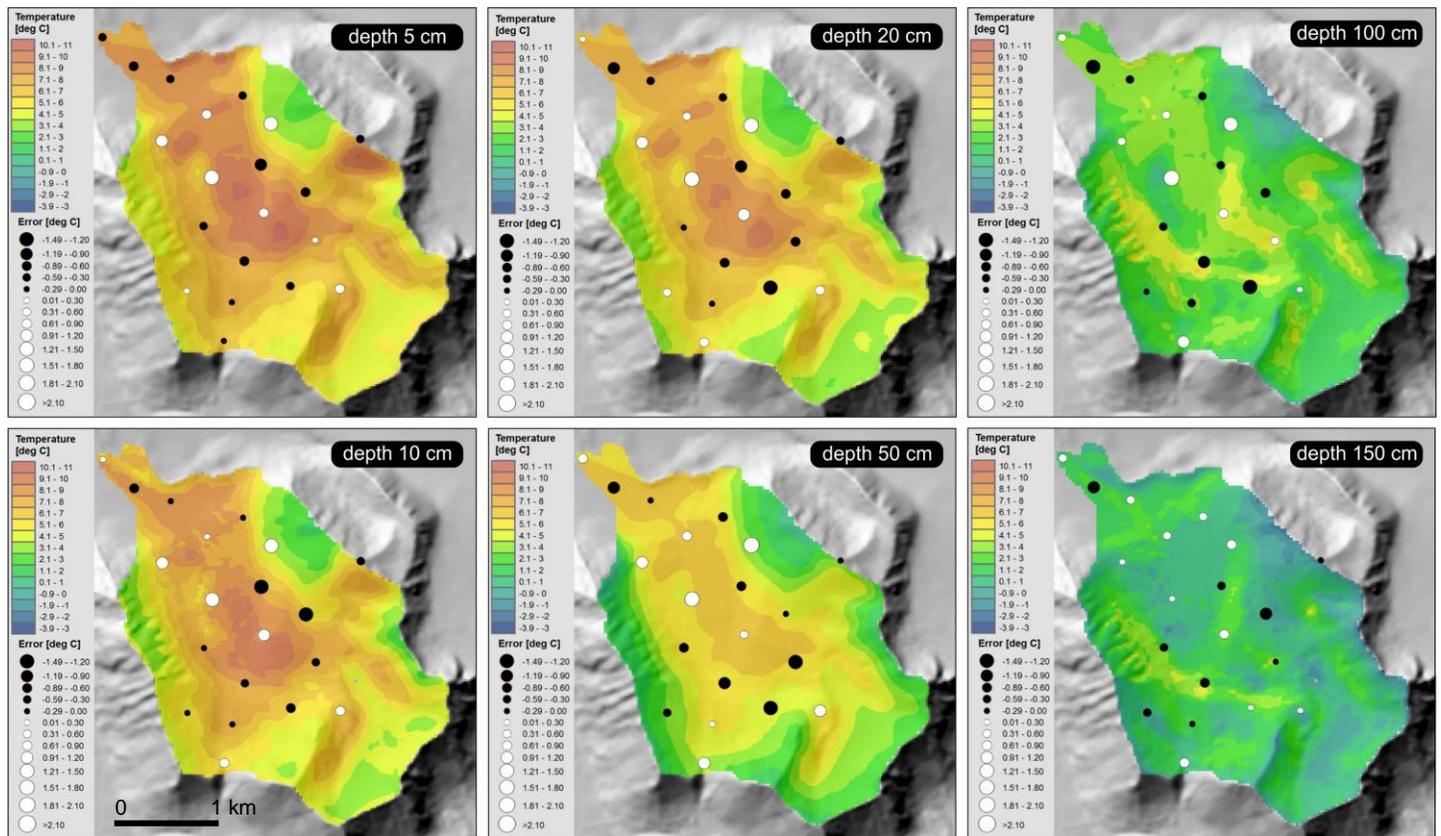| Depth [cm]	Model	Auxiliary variables	Adjusted R^2	Standard Error
5	GWR	LST, ValDepth	0.64	0.94
10	GWR	LST, ValDepth, COS_AS	0.60	1.00
20	GWR	LST, ValDepth	0.56	1.06
50	GWR	RelSlPos, LST	0.42	1.24
100	GWR	RelSlPos, LS, LST	0.54	1.10
150	GWR	RelSlPos, LS, COS_AS , LST	0.64	0.75

Figure 4.   Ground average temperatures modeled using geographically weighted regression (GWR).

arity of the spatial process. In no case did the residuals of the model have a statistically significant positive autocorrelation, so there was no basis for extending the regression model to the residual kriging.

IV. Conclusions

The conducted spatial analysis and modelling of soil thermal conditions allow us to point out several main conclusions:

1. On and near the surface (0 and 5 cm depth) the temperature is not correlated with any of the land surface parameters. The only statistically significant correlation ($p < 0.05$) occurs with LST (from 2017-08-3, around noon). This shows that neither topography nor variations in height, followed by air temperature, but properties of the ground, its thermal features (conductivity and heat capacity), ground moisture, tundra vegetation, occurrence of snow patches etc. are likely to determine the temperature variation in the subsurface.

2. A significant positive correlation of ground temperature (TG) with LST is maintained to a depth of 50 cm, with the correlation decreasing with depth. At 100 cm and 150 cm the correlation is irrelevant. From 10 cm deep there is a significant negative correlation with elevation, expressed both in altitude (H) and various parameters describing the relative height (VertDist, RelSlPos). The correlation increases with depth up to 50 cm, and then weakens, but remains still significant and strong ($R < -0.5$). The TPI index always has a negative, though insignificant correlation with TG (the strength of the relationship grows with depth). This means that the more convex form of the terrain, the lower the temperature than at analogous depths in concave forms. TG shows a positive correlation with TWI (the more potentially the wetter, the warmer). Together with depth, the strength of the relationship increases to -50 cm and then decreases. TG correlation with TWI is only significant at the -50 cm depth.

3. In multivariable regression models, the dependence of TG on LST and height is confirmed. However, because LST is correlated with H, the model included variables expressing relative height (ValDepth, RelSlPos), which are not significantly correlated with LST. From -50 cm, the relative height (RelSlPos) determines the distribution of TG more strongly than above.

4. Variability of TG without inclusion of LST in the model is less explained than with the introduction of LST. Introducing LST into the model necessitated the removal of altitude and insolation, but such a two-factor geo-weighted model (GWR) allowed to explain as much as 56% of TG variation at the depth of 20 cm.

6. The degree of explanation in the cases considered was the highest at the surface (-5 cm) and at the biggest depth (-150 cm) and accounted for 64% of the variability of the observed TG. The GWR model at -50 cm explained the variation in ground temperature only in 42%. Along with the decrease in the explanation level, the magnitude of the standard estimation error also increased.

References

[1] Etzelmueller, B., Schuler, T.V., Isaksen, K., Christiansen, H.H., Farbrot, H. and R. Benestad, 2011. "Modeling the temperature evolution of Svalbard permafrost during the 20th and 21st century", The Cryosphere, 5, 67–79.

[2] Harris, C., Arenson, L.U., Christiansen, H.H., Etzelmüller, B., Frauenfelder, R., Gruber, S., Haeberli, W., Hauck, C., Hölzle, M., Humlum, O., Isaksen, K., Kääb, A., Kern-Lütschg, M.A., Lehning, M., Matsuoka, N., Murton, J.B., Nötzli, J., Phillips, M., Ross, N., Seppälä, M., Springman, S.M. and D.V. Mühll, 2009. "Permafrost and climate in Europe: Monitoring and modelling thermal, geomorphological and geotechnical responses", Earth-Science Reviews, 92, 3–4, 117–171.

[3] Leszkiewicz, J. and Z. Caputa, 2004. "The thermal condition of the active layer in the permafrost at Hornsund, Spitsbergen", Polish Polar Research, 25, 3-4, 223–239.

[4] Dolnicki, P., Grabiec, M., Puczko, D., Gawor, Ł., Budzik, T. and J. Klementowski, 2013. "Variability of temperature and thickness of permafrost active layer at coastal sites of Svalbard", Polish Polar Research, 34, 4, 353–374.

[5] Isaksen, K., Sollid, J.L., Holmlund, P. and C. Harris, 2007. "Recent warming of mountain permafrost in Svalbard and Scandinavia", Journal of Geophysical Research, 112, F02S04.

[6] Rachlewicz, G. and W. Szczuciński, 2008. "Changes in thermal structure of permafrost active layer in a dry polar climate, Petuniabukta, Svalbard", Polish Polar Research 29, 3, 261–278.

[7] Sobota, I. and M. Nowak, 2014. "Changes in the dynamics and thermal regime of the permafrost and active layer of the High Arctic coastal area in North-West Spitsbergen, Svalbard", Geografiska Annaler, Ser.A, Physical Geography, 96, 227–240.

[8] Norwegian Polar Institute, 2014. Terrengmodell Svalbard (S0 Terrengmodell) [Data set], https://doi.org/10.21334/npolar.2014.dce53a47

[9] Walawender, J.P., Hajto, M. and P. Iwaniuk, 2012. "A new ArcGIS toolset for automated mapping of land surface temperature with the use of LANDSAT satellite data", Conference: Geoscience and Remote Sensing Symposium (IGARSS), 2012 IEEE International, 4371–4373.

[10] Barsi, J.A., J.L. Barker, J.R. Schott, 2003. "An Atmospheric Correction Parameter Calculator for a Single Thermal Band Earth-Sensing Instrument". IGARSS03, 21–25 July 2003, Centre de Congres Pierre Baudis, Toulouse, France (https://atmcorr.gsfc.nasa.gov/).

[11] Szymanowski, M., Kryza, M. and W.A. Spallek, 2013. "Regression-based air temperature spatial prediction models: An example from Poland", Meteorologische Zeitschrift 22(5), 577 - 585.